Article:
Amphlett, J.T.M., Choi, S., Parry, S.A. et al. (2020) Insights on uranium uptake mechanisms by ion exchange resins with chelating functionalities: Chelation vs. anion exchange. Chemical Engineering Journal, 392. 123712. ISSN: 1385-8947

https://doi.org/10.1016/j.cej.2019.123712

Determination of Uranium Coordination Environment on Ion Exchange Resins in Saline and Non-Saline Environments

J. T. M. Amphlett[a,b], S. A. Parry[c], C. A. Sharrad[a], S. Choi[b] *M. D. Ogden[d]

[a] School of Chemical Engineering and Analytical Science, The University of Manchester, Oxford Road, Manchester, M13 9PL, United Kingdom.

[b] Nuclear and Quantum Engineering Department, Korea Advanced Institute of Science and Technology (KAIST), Daejeon, South Korea

[c] Diamond Light Source Ltd., Diamond House, Harwell Science and Innovation Campus, Didcot, Oxfordshire OX11 0DE, United Kingdom.

[d] Separations and Nuclear Chemical Engineering Research (SNUCER), Department of Chemical and Biological Engineering, The University of Sheffield, Mappin Street, Sheffield, S1 3JD, United Kingdom.

*Corresponding author's email: m.d.ogden@sheffield.ac.uk

Abstract

Extended X-ray absorption fine structure (EXAFS) analysis has been successfully used to determine the coordination environment and therefore uptake mechanism towards the uranyl cation for a selection of commercially available ion exchange resins in non-saline and saline conditions ($[Cl^-]$ = 22.7 g L^{-1}, 0.64 M) similar to those found in sea water. The resins tested were Purolite S985, S910 and S957, Dowex M4195, Ps-EDA, Ps-DETA and Ps-PEHA, which contain polyamine, amidoxime, mixed sulfonic/phosphonic acid, bispicolylamine, ethylenediamine, diethylenetriamine and pentaethylenehexamine functional groups, respectively. Purolite S910 and S957 were both found to extract the uranyl cation through a chelation mechanism. The uranium coordination environment on uranyl loaded Purolite S910 was found to be either tetra- or hexa-coordinate in the equatorial plane, with two a 2:1 ratio of amidoxime:uranium in the fit suggesting either monodentate or η^2 coordination via 2 amidoxime groups. The uranium environment for uranyl loaded Purolite S957 was found to be tetra-coordinate in the equatorial plane, with both sulfonic and phosphonic acid groups

being involved in sorption. The presence of chloride in the loading solution had no effect on the uranyl coordination environment observed on any of the resins. A variation on the F-test was applied to the addition of a sulfur atom from a sulfate group to the fits for Purolite S910 and S957. The addition of this scattering path to the EXAFS fit was only found to be significant for the fit of uranyl bound to Purolite S957 under saline conditions. In contrast, Dowex M4195, Purolite S985, Ps-EDA, Ps-DETA and Ps-PEHA exhibited an anion exchange mechanism for uranyl uptake as the corresponding EXAFS data were fit to a $[UO_2(SO_4)_3]^{4-}$ structure.

1. Introduction

Nuclear power is becoming an increasingly attractive sustainable energy source to cope with population growth and climate change. With this in mind, many countries around the world are investing in new nuclear. There are currently over 60 reactors being constructed and many more in planning, with a predicted rise of up to 200% in global electricity produced from nuclear by 2050.[1] As the number of reactors increases, so will the demand for uranium. Uranium mining requires vast quantities of fresh water, which can be problematic. Many mines are in arid environments, and the use of fresh water in mine processing circuits can put a strain on drinking supplies for local populations. There are also large costs involved in purifying wastewater from these processing circuits for release back into the environment and the option to desalinate low quality waters for use in processing is expensive and energy intensive. In order to meet uranium demands for future nuclear energy requirements in an economically and environmentally sustainable way, new extraction technologies need to be developed to allow the use of low quality waters for uranium recovery, such as those containing high saline. An example of this would be seawater, which has an average chloride concentration of 22.7 g L^{-1} (0.64 M).

The uranium mining industry has become heavily reliant on the use of strong base anion (SBA) exchange resins for the extraction of uranium. However, these conventional SBA resins are not compatible with the use of low quality waters, due to the suppression of ion exchange (IX) at high ionic strengths.[2,3] These streams are reported to be more compatible with weak base anion (WBA) exchange resins and chelating IX resins than traditional anion exchangers.[3–6] A fundamental understanding of the behaviour of UO_2^{2+} towards these resin types in sulfate processing liquors with/without high chloride content is lacking, as is structural data for the exchanged U species on their surface. Understanding the speciation in

these systems could result in more effective uranium milling flowsheets, which can tolerate these anions and could lead to engineering their implementation in uranium recovery for mining applications and environmental waste management strategies. This enhanced understanding of uranium recovery could also be transferred to the extraction of other high value, critical metals, such as rare earths and platinum group metals, ultimately allowing for the maintenance and spreading of the high quality of life associated with advanced technologies enjoyed by many, which relies heavily on these elements.

WBA resins differ from SBA resins due to their different functionalities. SBA resins always contain a quaternary ammonium group, and are therefore always positively charged.[7] Charge balance is typically maintained by the presence of readily exchangeable anions found in the solution environments the resins are exposed to, such as sulfate. However, WBA resins are generally functionalised with primary, secondary and/or tertiary amines, and therefore their ability to become charged is dependent upon solution chemistry and their pK_a values. They function in the same way as SBA resins, as when they become protonated they can exchange associated anionic co-ions with aqueous anions. In the case of uranyl recovery from acidic sulfate conditions, the extracted species is generally believed to be $[UO_2(SO_4)_3]^{4-}$. However, EXAFS studies by Moon *et al.* on uranyl loaded tertiary amine WBA resin, Dowex Monosphere 77, from solutions with $[Cl^-]$ of 0 – 5 M, 1 – 2 M and 3 – 5.8 M ($[SO_4^{2-}]$ = 0.25 M, $[UO_2^{2+}]$ = 4 mM) have shown the extracted species to be $[UO_2(SO_4)_2(H_2O)]^{2-}$, $[UO_2(SO_4)Cl.(H_2O)_2]^-$ and $[UO_2Cl_4]^{2-}$, respectively.[6] A difference in uranyl speciation was also observed between the aqueous and resin phases.

Chelation resins generally have molecular functionalities, attached to the surface of the bulk resin matrix, consisting of multiple ligating atoms that can coordinate to a metal ion resulting in the formation of a chelate ring. These chelate rings are typically thermodynamically favoured over equivalent coordination complexes with ligands that have only one binding site due to entropic considerations described by the chelate effect.

There are many molecules capable of forming multidentate complexes with uranium in aqueous and organic phases, many of which could conceivably be grafted onto a solid to produce an IX resin.[8] However, there are only a relatively small number of commercially available resins with molecular functionalities that are capable of chelating to metal ions, which could be applied to uranium extraction. However, despite these resins being marketed as “chelation resins” there is little direct evidence to indicate these resins do actually chelate

metal ions. We have recently shown, by the application of EXAFS spectroscopy, that a series of polyamine functionalised resins, capable of chelating metal ions, actually perform as anion exchangers for uranyl from sulfate solutions at pH 2.[9] In these examples, uranyl in the form of an anionic complex, $[UO_2(SO_4)_3]^{4-}$, binds to these resins by an ionic interaction with protonated amines on the resin. The branched polyamine functionalised resin Purolite S985 resin has also been shown to act as an anion exchanger under similar conditions.[9]

The work aims to establish uranyl speciation upon a selection of loaded WBA and chelation resins from solutions containing saline concentrations similar to those in sea water (i.e. $[Cl^-]$ = 22.7 g L^{-1}), and therefore the mechanisms by which these resins uptake uranyl by low quality waters. This speciation will be compared against resins prepared from analogous loadings performed under fresh water conditions. The chosen WBA resins for this work are three in house synthesised resins (Ps-EDA, Ps-DETA, Ps-PEHA) and Purolite S985 (Fig.1), and the chosen commercial chelation resins are Purolite S910, Purolite S957 and Dowex M4195 with amidoxime, mixed sulfonate/phosphonate and bispicolylamine functionalities, respectively (Fig.2).[9] The establishment of the mechanism by which these resins uptake uranyl are then compared to process performance parameters in order to identify criteria that can be used for the selection of IX resin that provide give optimum extraction properties based upon likely solution composition.

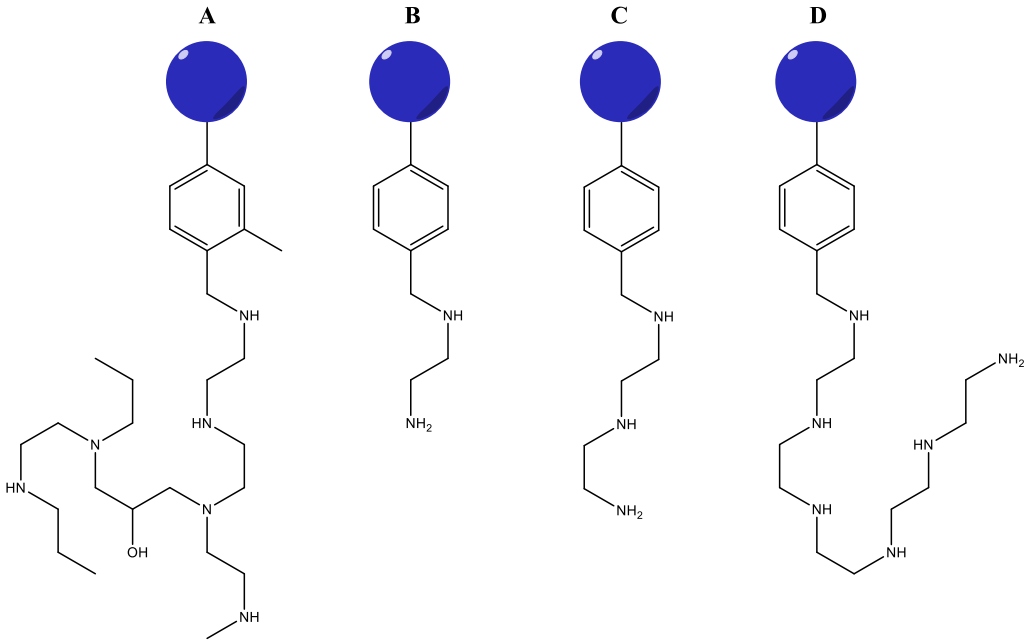

Figure 1. Functional groups of Purolite S985 (A), Ps-EDA (B), Ps-DETA (C) and Ps-PEHA (D)

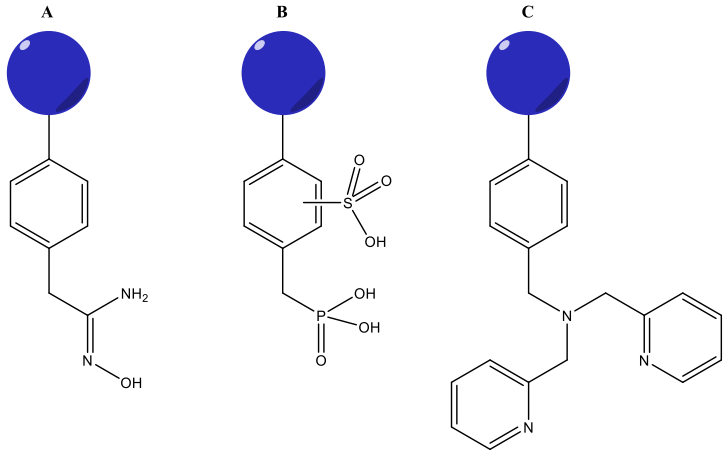

Figure 2. Functional groups of Purolite S910 (A), Purolite S957 (B) and Dowex M4195 (C)

2. Experimental

2.1. Reagents and Stock Solutions

Dowex M4195 IX resin was purchased from Sigma Aldrich, with all other commercial resins kindly being supplied by Purolite. Manufacturer resin specifications are shown in Tables 1, 2, 3 and 4. In house produced WBA resins were synthesised via previously established methods.[9] Resins were preconditioned by contacting with H_2SO_4 (1 M) for 24 hours, with a resin:acid ratio of 1:10 (v:v). Aqueous uranyl sulfate solutions were supplied by the University of Sheffield.

Table 1. Manufacturer specifications for chelating resin Dowex M4195

Parameter	Value
Functionality	Bis-picolylamine
Matrix structure	Polystyrene crosslinked with divinylbenzene, macroporous
Copper loading capacity	35 – 42 g L^{-1}
Form	Weak base/partial H_2SO_4 salt
Moisture	40 – 60 %

Table 2. Manufacturer specifications for chelating resin Purolite S957

Parameter	Value
Functionality	Phosphonic and sulfonic acid
Matrix structure	Polystyrene crosslinked with divinylbenzene, macroporous
Iron loading capacity	18 g L^{-1}
Form	H^+
Moisture	55 – 70 %

Table 3. Manufacturer specifications for chelating resin Purolite S910

Parameter	Value
Functionality	Amidoxime
Matrix structure	Polyacrylic crosslinked with divinylbenzene
Copper loading capacity	40 g L^{-1}
Form	Free base
Moisture	52 – 60 %

Table 4. Manufacturer specifications for WBA resin Purolite S985

Parameter	Value
Functionality	Polyamine
Matrix structure	Macroporous polyacrylic crosslinked with divinylbenzene
Total capacity	2.3 eq L^{-1}
Form	Free base
Moisture	52 – 57 %

2.2. Uranium Uptake

All resin was ground to a fine powder before uptake experiments to prevent artifacts in the EXAFS data due to the imperfect packing of spheres, and to remove the need to grind uranium loaded resins post contact. Ground resin (4 g) was contacted with a uranyl solution (1 g L^{-1} U, 50 mL) in sulfuric acid (pH 2). Uptake was also performed from the same uranyl solutions but with the addition of chloride (22.7g L^{-1} Cl, 0.64 M) as sodium chloride. [SO_4^{2-}] was kept constant at 1.4 g L^{-1} (14.6 mM).

2.3. EXAFS Experiments

After contacting with uranyl solution, the loaded resin was dewatered and transferred into cylindrical cryo-tubes. These tubes were vacuum packed in plastic and left this way for

measurement. The same was done for samples of non-saline and saline solution which had not been contacted with resins. Uranium L_{III}-edge X-ray absorption spectra were recorded in transmission mode on beamline B18 at the Diamond Light Source operating in a 10 min top-up mode for a ring current of 299.6 mA and an energy of 3 GeV. The radiation was monochromated with a Si(111) double crystal, and harmonic rejection was achieved through the use of two platinum-coated mirrors operating at an incidence angle of 7.0 mrad. The monochromator was calibrated using the K-edge of an yttrium foil, taking the first inflection point in the Y-edge as 17038 eV. Multiple spectra were recorded for each sample, with the sample being moved between each scan of a single spectrum as having the beam incident on one area of the sample for too long was seen to decompose the resins.

2.4. EXAFS Data Analysis

X-ray absorption spectra were aligned, combined and normalised using the Athena software package. Fits of the EXAFS data were performed using FEFF database via the Artemis software package. The only parameters fixed for each fit were the occupancies of each shell, allowing for the refinement of the amplitude factor (amp) and dE_0 for the entire k range, and U-X interatomic distances (R) and Debye-Waller factors (σ^2) for each individual scattering path.

A way determining if the addition of extra scattering paths to an EXAFS fit is relevant and/or statistically significant further than just comparing the goodness of fit parameters is to employ a variation of the F-test.[10,11] This test employs the R-factor produced in the fitting process for the two fits being compared to produce a confidence interval which allows an understanding of if one fit is significantly better than the other. The confidence interval is calculated using Eq 2-4, where F is the result of the F-test, R_1 and R_0 are the R-factors for the worse and better fits respectively, n is the number of independent points in the fit, m is the number of variables used in the fit, b is the difference in the number of parameters used in fits of R_1 and R_0 (known as the dimension of the fit), I_X is the incomplete beta function and α is the confidence interval. The confidence interval must be greater than 67%, but ideally greater than 95%, for the R_0 fit to be considered significantly better than R_1.

$$F = \frac{(R_1^2 - R_0^2)/b}{R_0^2/(n-m)} = \left[\left(\frac{R_1}{R_0}\right)^2 - 1\right] \times \frac{n-m}{b} \qquad \textbf{Eq.2}$$

$$\alpha = 1 - I_X\left(\frac{n-m}{2}, \frac{b}{2}\right) \quad \textbf{Eq.3}$$

$$X = \left(\frac{n-m}{n-m+bF}\right) \quad \textbf{Eq.4}$$

3. Results and Discussion

U L_{III}-edge EXAFS spectra were collected of uranyl-containing aqueous phases for both non-saline ([U] = 1 g L^{-1}, [$(SO_4)^{2-}$] = 1.4 g L^{-1}, pH 2.0) and saline conditions ([U] = 1 g L^{-1}, [$(SO_4)^{2-}$] = 1.4 g L^{-1}, [Cl^-] = pH 2), and of numerous ion exchange resins consisting of various chelating functionalities upon which uranyl was loaded from both the aqueous phases studied. Experimental data in R- and K-space are shown in the supplemental information (Fig. S1 and S2). Multiple fits of each EXAFS profile were performed using likely uranyl coordination environments across various numbers of sulfate, chloride and water ligands. Fits were also attempted against sulfate containing coordination environments taking in consideration the possibility that sulfate could act either as a bidentate or monodentate ligand. Coordination environments that provide the best fit/s for each EXAFS profile are discussed below. None of these studies provided any evidence for the presence of multimetallic uranyl molecular species by ligands acting in a bridging mode or any species that may be considered as oligomeric.

3.1. Aqueous solutions

The collected EXAFS spectra of UO_2^{2+} in non-saline and saline solution environments show obvious differences, suggesting that Cl^- has an effect on the uranyl (at 1 g L^{-1} U) coordination environment between chloride concentrations of 0 and 22.7 g L^{-1} (0 – 0.64 M). This agrees with EXAFS data published by Moon *et. al.*, with different chloro-/sulfato-/mixed chloro- sulfato- complex species being identified with varying [Cl^-] (0.5 – 1 M) and [SO_4^{2-}] (0 – 0.24 M).[6] These uranyl coordination environments were used as a guide for our fitting models.

The non-saline spectrum was successfully fitted with a uranyl species coordinated by 6 oxygen atoms in the equatorial plane (Fig. 3). Attempts to include sulfur (sulfate) atoms in the fit did result in good fitting parameters, resulting in a $[UO_2(SO_4)_3]^{4-}$ species. However, the addition of these atoms to the fit is questionable due to the weak signal at R > 2.5

Å. This is not consistent with the data of Moon *et. al.*, which showed equatorially penta-coordinate UO_2^{2+} to be the majority species present across all [SO_4^{2-}] and [Cl^-] tested. However, the lack of competition with Cl^- in these samples for uranyl binding likely explains this difference. Equatorial U-O distances of 2.31 – 2.43 are consistent with H_2O and bidentate sulfate ligands.[6,12]

For the EXAFS spectrum obtained of the saline solution, attempts were made to fit the profile to uranyl coordination environments that included chloride atoms into the fit, resulting in a fit of a uranyl molecule which is 5-coordinate in the equatorial plane (4 O, 1 Cl; Fig. 3). As with the non-saline environment, attempts were made to include sulfur atoms in the fit ($[UO_2(SO_4)_2Cl]^{3-}$ species) to discern the identity of the oxygen atoms, but again, the weak signal R > 2.5 Å renders this questionable (even though fitting parameters were adequate). The fitted equatorial region of 4 O's and a Cl agrees with the data collected by Moon *et. al.*, aiding in validating our fitting procedure and alluding to the preferential formation of UO_2^{2+}-chloro species over pure sulfate coordination. As with the non-saline spectrum, the U-O equatorial distances are consistent with H_2O and bidentate SO_4^{2-} ligands. In addition, the U-Cl^- distance is in strong agreement with those observed by Moon *et. al.*.

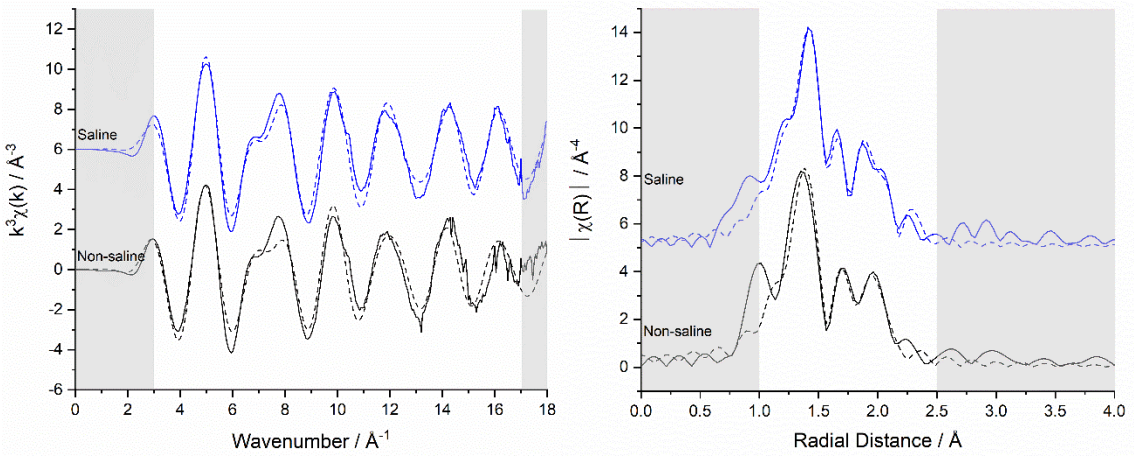

Figure 3. Uranium L_{III}-edge EXAFS spectra in R- and K-space for uranyl in non-saline (left) and saline (right) environments. Non-saline data is fit with an equatorially hexa-coordinate species using only O atoms, saline data is fit with an equatorially penta-coordinate species, using 4 O atoms and 1 Cl atom. The unshaded region represents the fitting window, solid and dashed lines show the data and fits, respectively.

Table 5. U L_{III}-edge EXAFS fitting parameters for data from uranyl in non-saline and saline environments.

	Scattering Path	N	R / Å	σ^2	dE_0 / eV	amp	R-Factor
Non-Saline	U-O_{axial}	2	1.78	0.00135	-0.333	0.832	0.0255
	U-$O_{equatorial}$	4	2.43	0.00449			
	U-$O_{equatorial}$	2	2.31	0.00530			
Saline	U-O_{axial}	2	1.77	0.00121	0.462	0.874	0.0072
	U-$O_{equatorial}$	2	2.43	0.00313			
	U-$O_{equatorial}$	2	2.34	0.00263			
	U-$Cl_{equatorial}$	1	2.69	0.00592			

The major difference between the non-saline and saline UO_2^{2+} complexes is the change from 6- to 5-coordination in the equatorial plane. It is unclear what explicitly drives this change, however, it must be due to the presence of Cl^-, which is 43.8 times more concentrated than SO_4^{2-} in the saline environment. As it was not possible to include sulfur atoms in our fits it is difficult to discuss these differences in terms of binding strengths of sulfate ligands vs. chloride ligands, though it is likely that these interactions are important in determining this behaviour.

3.2. Polyamine WBA Resins

Presented EXAFS data of the uranyl loaded WBA resins with polyamine functionalities (Figure 1) were contacted from the saline environment only, with data for the same resins loaded with uranyl from a non-saline environment being reported previously.[9] All collected spectra exhibited similar profiles, indicating that the same uranyl surface species is found upon all the polyamine WBA resins studied here. Attempts were made to fit these EXAFS profiles to the $[UO_2(SO_4)_3]^{4-}$ species likely found in the loading solutions, and the $[UO_2(SO_4)_2.H_2O]^{2-}$ species identified by Moon *et al.* bound to the tertiary amine functionalised WBA resin Dowex Monosphere 77 when uranyl was loaded from aqueous solutions where $0 \leq [Cl^-] \leq 0.5$ M. Attempts to fit the EXAFS profiles to the $[UO_2(SO_4)_2.H_2O]^{2-}$ species returned poor goodness of fit parameters. The best fits for the EXAFS spectra collected from all the polyamine WBA resins where uranyl was loaded from saline conditions were obtained using the $[UO_2(SO_4)_3]^{4-}$ species (Fig.4, Table 6). Two U-O_{eq} shells were included in the fit to avoid

over parameterisation (as with the aqueous samples), and due to the presence of two distinct peaks in the EXAFS profiles either side of 2 Å, an area known to correspond to the equatorial uranyl coordination environment. The U-O_{eq} interatomic distances between 2.34 Å and 2.49 Å, though longer than those seen in the studied aqueous samples, are consistent with bidentate sulfate coordination environments previously reported for U-sulfato aqueous and surface species.[6,14] The EXAFS profiles of the same resins loaded with uranyl from non-saline solutions also exhibited best fits using the $[UO_2(SO_4)_3]^{4-}$ species.[9]

Minimal differences were observed in the refined interatomic distances obtained from the EXAFS profiles between the different types of WBA and the different loading solutions. This shows that there is no impact of chloride on uranyl speciation on these polyamine WBA resins for loading solution conditions where $0 \leq [Cl^-] \leq 0.64$ M. A change in uranyl coordination environment upon extraction is observed from the saline media, via the exchange of a chloride with a sulfate ligand. There is no indication that the polyamine functionalities upon these WBA resins exhibit chelation, or any coordination bonding, to uranyl under the conditions studied in this work. These polyamine WBA resins therefore act as anion exchangers for uranyl sulfate species from non-saline and saline conditions similar to sea water, despite possessing functionalities that could potentially form a chelation complex with the uranyl ion.

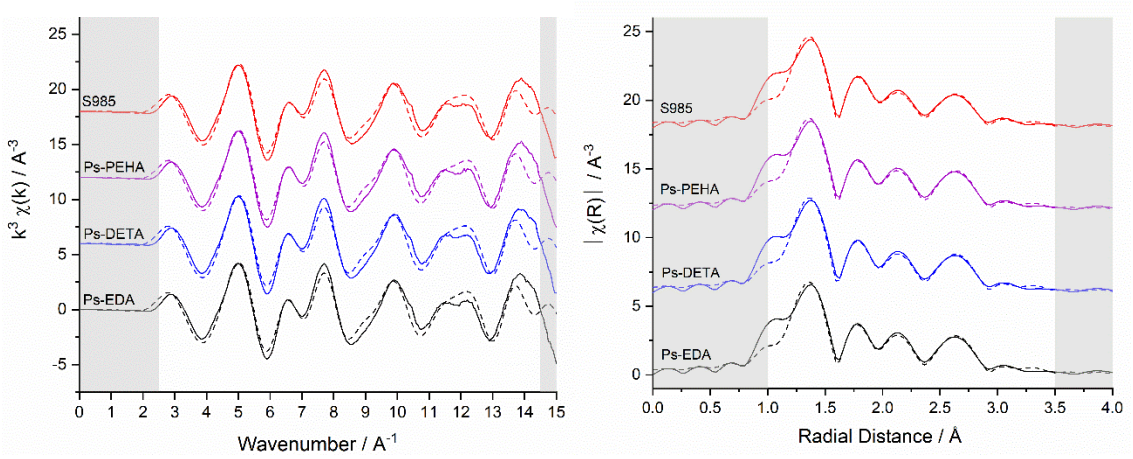

Figure 4. Uranium L_{III}-edge EXAFS spectra in K-space (left) and R-space (right) for uranyl loaded Ps-EDA, Ps-DETA, Ps-PEHA and Purolite S985 in saline media, fit with a $[UO_2(SO_4)_3]^{4-}$ species. The unshaded region represents the fitting window, solid and dashed lines show the data and fits, respectively.

Table 6. U L_{III}-edge EXAFS fitting parameters of data from uranyl loaded Ps-EDA, Ps-DETA, Ps-PEHA and Purolite S985 from acidic saline media.

	Scattering Path	N	R / Å	σ^2	dE_0 / eV	amp	R-Factor
Purolite S985	U - O_{axial}	2	1.79	0.00234	1.642	0.901	0.0202
	U - $O_{equatorial}$	4	2.49	0.00482			
	U - $O_{equatorial}$	2	2.34	0.00292			
	U - S	2	3.11	0.00234			
	U - S	1	3.26	0.00193			
Ps-EDA	U - O_{axial}	2	1.79	0.00213	1.471	0.902	0.0208
	U - $O_{equatorial}$	4	2.49	0.00422			
	U - $O_{equatorial}$	2	2.34	0.00284			
	U - S	2	3.11	0.00141			
	U - S	1	3.25	0.00108			
Ps-DETA	U - O_{axial}	2	1.79	0.00220	1.676	0.928	0.0197
	U - $O_{equatorial}$	4	2.49	0.00446			
	U - $O_{equatorial}$	2	2.34	0.00278			
	U - S	2	3.11	0.00166			
	U - S	1	3.25	0.00113			
Ps-PEHA	U - O_{axial}	2	1.79	0.00229	1.661	0.909	0.0203
	U - $O_{equatorial}$	4	2.49	0.00433			
	U - $O_{equatorial}$	2	2.34	0.00301			
	U - S	2	3.11	0.00144			
	U - S	1	3.25	0.00105			

3.3. Dowex M4195

Dowex M4195 is a WBA resin containing bispicolylamine (BPA) functionalities which are capable of chelating to metal cation species. The obtained EXAFS profiles of this resin when loaded with uranyl from saline and non-saline environments are similar to each other and to those obtained from the uranyl loaded polyamine WBA resins. Attempts to fit the EXAFS data of the uranyl loaded Dowex M4195 resin with a uranyl ion chelated by BPA did not provide acceptable fits. The best fit for data obtained from both loading conditions was provided by the $[UO_2(SO_4)_3]^{4-}$ species (Fig.5, Table 7), as was the case for the uranyl loaded polyamine WBA resins.[10] Examinations of the produced radial distribution plots for uranyl loaded Dowex M4195 resin show that these too are very similar to those obtained for uranyl

loaded polyamine functionalised WBA resins from non-saline conditions.[9] This is in agreement with previously discussed U-O_{eq} and U-S interatomic distances. Fits of uranyl loaded Dowex M1495 resin from saline conditions incorporating Cl^- were attempted, but again produced unacceptable fitting parameters. Potentiometric titration data has shown that Dowex M4195 is able to become dicationic, with protonation constants pK_1 and pK_2 determined as 4.13 and 2.1, respectively.[15,16] Taking into account charge neutralisation constraints, this would allow for the interaction of two fully protonated BPA groups with the sorbed $[UO_2(SO_4)_3]^{4-}$ species, or one fully protonated BPA group extracting the $[UO_2(SO_4)_3]^{4-}$ species with aqueous cations associated with it.

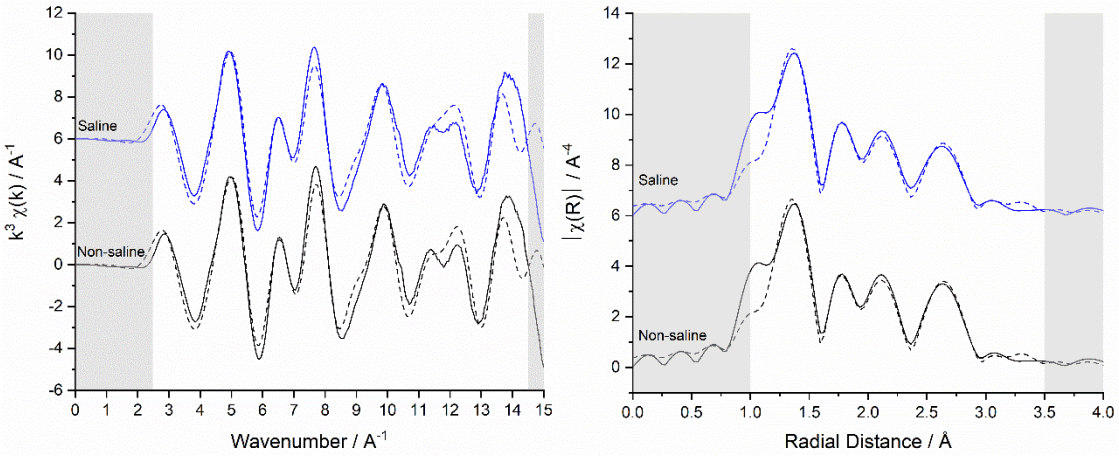

Figure 5. Uranium L_{III}-edge EXAFS spectra in K-space (left) and R-space (right) for uranyl loaded Dowex M4195 from non-saline and saline environments, fit with a $[UO_2(SO_4)_3]^{4-}$ species. The unshaded region represents the fitting window, solid and dashed lines show the data and fits, respectively.

Table 7. U L_{III}-edge EXAFS fitting parameters of data from uranyl loaded Dowex M4195 from non-saline and saline conditions. *Values linked to other multiple scattering (MS) paths and were parameterised accordingly.

	Scattering Path	N	R / Å	σ^2	dE_0 / eV	amp	R-Factor
Non-Saline	U-O_{axial}	2	1.79	0.00219	1.377	0.906	0.0204
	U-$O_{equatorial}$	4	2.50	0.00332			
	U-$O_{equatorial}$	2	2.36	0.00272			
	U-S	1	3.11	0.00707			
	U-S	2	3.24	0.00660			
	U-O_{axial} (MS)	2	3.58*	0.00447*			
Saline	U-O_{axial}	2	1.79	0.00227	1.617	0.901	0.0218
	U-$O_{equatorial}$	4	2.50	0.00400			
	U-$O_{equatorial}$	2	2.35	0.00320			

	U-S	1	3.11	0.00320	
	U-S	2	3.25	0.00165	
	U-O_{axial} (MS)	2	3.58*	0.00447*	

The EXAFS data from uranyl loaded Dowex M4195 has been fit with a $[UO_2(SO_4)_3]^{4-}$ coordination environment, arising not from chelation, but from an anion exchange mechanism. This uptake mechanism towards uranyl agrees with data published for polyamine functionalised IX resins produced in industry and academia, where the same $[UO_2(SO_4)_3]^{4-}$ structural motif has been reported, as well as other anion exchange species ($[UO_2(SO_4)_2.H_2O]^{2-}$, $[UO_2ClSO_4]^-$and $[UO_2Cl_4]^{2-}$) observed on resins loaded from mixed chloride/sulfate conditions.[6,9] The addition of Cl^- groups to the model was attempted to fit the loaded resin from the saline environment but this gave goodness of fit parameters that were worse compared to those obtained from the tris(sulfato) model. It is likely that the Cl^- concentration (22.7 g L^{-1}, 0.64 M) was not sufficiently high enough to form an appreciable amount of chloride coordinated uranyl species, such as $[UO_2ClSO_4]^-$, which was observed by Moon *et al*. to be the dominant uranyl species extracted from mixed sulfate-chloride media between 1 and 3 M Cl^-.[6]

3.4. Purolite S910

Purolite S910 is marketed as a chelating resin containing the amidoxime functionality (Figure 2), for precious metals recovery and chromic acid purification. The produced EXAFS spectra of uranyl loaded Purolite S910 resin differ markedly from those seen for the uranyl loaded M4195 and other polyamine resins, especially with the absence of a large peak at roughly 2.6 Å corresponding to U-S scattering paths.[6,9] Therefore, indicating that the uranyl coordination environment upon Purolite S910 resin is not $[UO_2(SO_4)_3]^{4-}$, as could be the case with an anion exchange mechanism, but another species, potentially formed via a chelation mechanism. There are multiple amidoxime-uranyl coordination structures that have been previously observed, from both EXAFS and X-Ray crystallography experiments, as well as computational methods, consisting of monodentate, bidentate, tridentate and η^2-bidentate

binding modes (Fig. 6).[17–20] These multiple possible structures make it challenging to assign the correct uranyl coordination environment/s for uranyl loaded Purolite S910 resin.

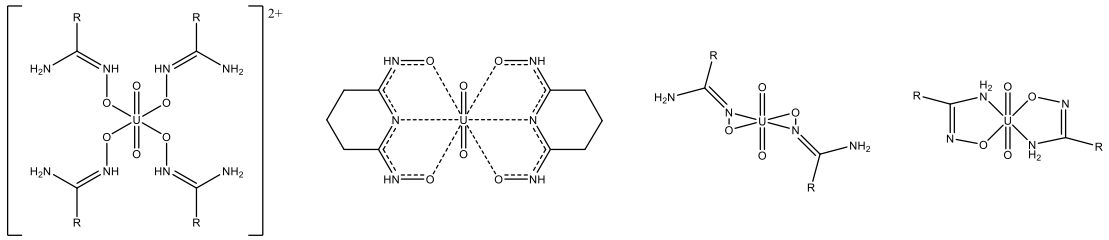

Figure 6.The possible binding modes of amidoxime/amidoximate molecules towards the uranyl cation (A = monodentate, B = tridentate chelate, C = η² chelate and D = bidentate chelate).[17–20]

Further to this, the close similarity between the spectra in both non-saline and saline conditions suggests a lack of influence of the Cl^- on uranyl coordination environment (Fig. 7). Using scattering paths from the crystal structures of possible tridentate and η^2-bidentate modes (B and C in Fig.6) to fit the EXAFS profiles for uranyl loaded Purolite S910 resin did produce acceptable R-factors, however, it was not possible to produce a fit with an amplitude correction factor below 1.65, suggesting these binding motifs were incorrect. The development of a fitting model with the use of a known uranium crystal structure where the amidoximate ligands coordinate to the metal ion in a monodentate manner through the oxygen donor (represented by A in Fig.6) did produce adequate goodness of fit parameters, giving a fit consisting of two amidoxime groups and two monodentate sulfate groups. This was the best fit for the data of uranyl loaded Purolite S910 obtained from both non-saline and saline conditions (Table 7).

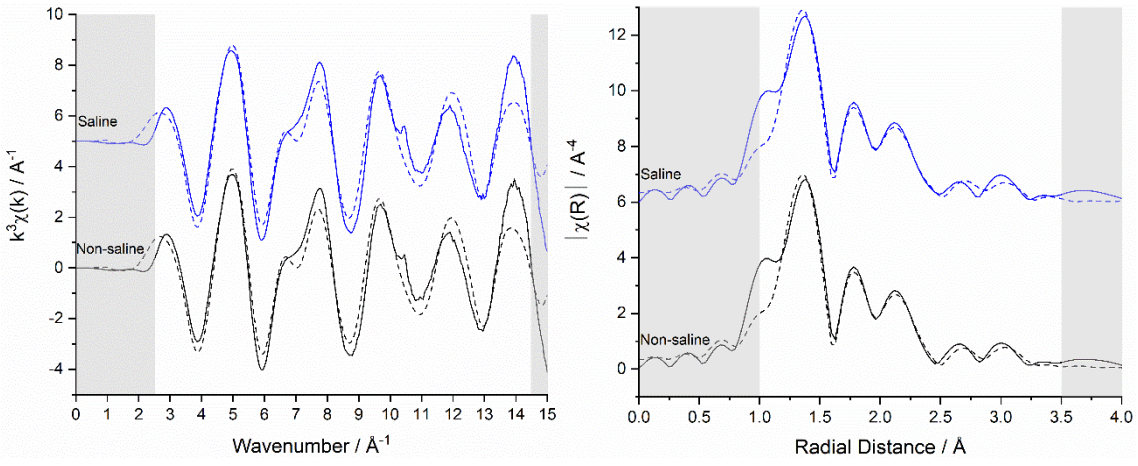

Figure 7. Uranium L_{III}-edge EXAFS spectra in K-space (left) and R-space (right) for uranyl loaded Purolite S910 from non-saline and saline environments, fit with uranyl bound in a monodentate manner to two amidoxime moieties and two monodentate sulfate groups. The unshaded region represents the fitting window, solid and dashed lines show the data and fits, respectively.

Table 8. Fitting parameters from the fitting of Purolite S910 in non-saline and saline conditions.

	Scattering Path	N	R / Å	σ^2	dE_0 / eV	amp	R-Factor
Non-Saline	U-O_{axial}	2	1.79	0.00243	4.253	1.089	0.0190
	U-$O_{equatorial}$	2	2.48	0.00189			
	U-$O_{equatorial}$	2	2.34	0.00339			
	U-N	2	2.87	0.00414			
	U-C	2	3.71	0.00678			
	U-S	2	3.65	0.00192			
Saline	U-O_{axial}	2	1.79	0.00247	4.002	1.089	0.0199
	U-$O_{equatorial}$	2	2.48	0.00196			
	U-$O_{equatorial}$	2	2.34	0.00368			
	U-N	2	2.87	0.00415			
	U-C	2	3.73	0.00184			
	U-S	2	3.66	0.00900			

Complexes with a 2:1 uranium:amidoxime ratio have been previously reported, with EXAFS and computational data published by Abney *et al*. suggesting this binding mode for uranium sorption from seawater onto amidoxime functionalised polymer fibres.[17] However, those results were postulated to show a bidentate chelated uranyl coordination environment, and showed different bond lengths to those produced from this fit (Table 9).

Table 8. Reported U-X interatomic distances for various uranium-amidoxime coordination environments NS and S are the non-saline and saline fits for uranyl binding to Purolite S910, respectively (X = O, N, C).[17–20]

	Monodentate[A]	η^2 [B]	Chelate[C]	NS[D]	S[E]
U-$O_{equatorial}$ / Å	2.30	2.38	2.43	2.34	2.34
	2.31	-	2.54	2.48	2.48
U-N / Å	3.21	2.40	2.56	2.87	2.87
	3.24	-	3.36		
	-	-	3.43		
U-C / Å	4.11	3.68	3.46	3.71	3.73
	4.19	-	3.48		

[A] Obtained by single crystal x-ray diffraction of $[UO_2(acetamidoxime)_4](NO_3)_2$.[18]
[B] Obtained by single crystal x-ray diffraction of $[UO_2(acetamidoxime)_2(MeOH)_2]$.[20]
[C] Obtained by single crystal x-ray diffraction of $[UO_2(glutarimidedioxime)_2(H_2O)]$.[19]

[D] This work using EXAFS.
[E] As immediately above.

The U-O_{eq} interatomic distance at 2.34 Å from the non-saline and saline fits is mid-way between those for the monodentate and η^2 binding modes presented from previous work on uranyl binding to acetamidoxime ligands.[18,20] This similarity is suggestive of these O_{eq} being associated with resin bound amidoxime moieties. Our data clearly shows a second O_{eq} environment, consisting of two O atoms at 2.48 Å. These are assigned to sulfate groups. A U-O bond distance of 2.48 Å is consistent with a bidentate sulfate binding mode, though fitted U-S distances are longer than would be expected for such a coordination environment. Alternatively, these oxygen atoms could be associated with HO^-, H_2O or H_3O^+ species present in solution, which is consistent with U-OH_2 interatomic distances reported for EXAFS fits of uranium sorbed on goethite, though the addition of sulfur atoms to the coordination model was seen to improve fitting parameters.[21] Monodentate sulfate groups have been reported with U-S distances around 3.56 Å in the aqueous phase, and from 3.58 to 3.62 Å in the solid phase.[6,12,22,23] These distances are much more consistent with those produced in our EXAFS fits.

The F-Test has been applied to assess the significance of the addition of the U-S scattering path for uranyl uptake onto Purolite S910 in both non-saline and saline conditions. The R-factors for the non-saline and saline fits without the U-S scattering path were the same, with a value of 0.0255. The only factor changing with the addition of this path is the amount of variables in the fit, going from 10 to 12. Results produced α values of 51% and 43% for the addition of the U-S path in the non-saline and saline environments respectively. This result does not allow for the definitive conclusion that the sulfur atoms are present. This fits with the U-$O_{equatorial}$ bond distance of 2.48 Å being longer than expected for a monodentate bound sulfate group, alluding to the conclusion that a different species may be more prevalent. However, it is still likely that there will be sulfate groups associated with some of the uranyl-amidoxime complexes, and the collected data is an average of multiple coordination environments. The lower α value for the saline fit compared to the non-saline one can be understood from the knowledge that there is much less sulfate in solution than chloride. If the interaction between the amidoxime bound uranyl and aqueous anionic groups is primarily based on electrostatics then there is a much higher probability that there would be chloride

atoms associated instead of sulfate, however, the addition of chloride into all fits greatly reduced the goodness of fit parameters.

Although the addition of U-S scattering paths improved the goodness of fit parameters, the results of the F-test do not allow for the conclusion that SO_4^{2-} groups are always bound to the central uranyl cation. It is likely that bound sulfate groups undergo a ligand exchange process with water and potentially other amidoxime O-donor groups, and the produced EXAFS signal is an average of these possible coordination environments. potentially including the bidentate chelate mode reported by Abney *et al.*, who also report the non-innocence of the adjacent amine group in uranyl binding.[17]

The observed U-N interatomic distance (2.87 Å) is unlike those seen for the reported literature structures shown in Table 8. It appears to be midway between the longer and shorter interatomic distances reported for the monodentate, $\eta^2$and chelate structures. This could again be due to steric effects of uranyl being bound to two separate amidoxime groups on the resin surface. The proximity of separate amidoxime groups on the matrix structure is not explicitly known. It is therefore plausible that this could cause steric effects causing interatomic distances to differ from those seen in the referenced crystal structures. The U-C interatomic distance however, is similar to that reported for the η^2 coordination environment, which could suggest a dominance of the η^2 mode. However, the other discussed U-X interatomic distances reported do not support that statement.

Another possibility that can justify these EXAFS fitting models is that there is more than one coordination environment present upon uranyl loaded Purolite S910 resin and the EXAFS signal is providing an average of these environments. Considering the multiple binding modes which have been reported for uranyl amidoxime/amidoximate complexes, this presence of multiple uranyl coordination species upon Purolite S910 is quite likely.

3.5. Purolite S957

Purolite S957 is a mixed sulfonic/phosphonic acid chelation resin, with collected EXAFS spectra of uranyl loaded forms of this resin (Fig. 8) showing almost no difference between that of the resin loaded from non-saline and that from saline conditions. The spectra, however, were different from those collected for the uranyl loaded forms of Dowex M4195, Purolite S910 and S985, and the linear polyamine WBA resins. Therefore the majority presence of the $[UO_2(SO_4)_3]^{4-}$ species could be discounted, especially with the lack of a large

peak in R-space at around 2.6 Å that would correspond to multiple U-S scattering paths. All potential chelation surface species can only contain oxygen atoms in the first equatorial shell, and fits were conducted with this in mind. Fits were attempted with O_{eq} occupancy varying from 4-6, with four O_{eq} atoms providing the best fit. Attempts were made to fit further shells containing sulfur and phosphorous atoms. The best fit was obtained using a model consisting of one phosphorous atom and two sulfur atoms outside of the immediate coordination sphere.

The statistical significance of the addition of the second U-S scattering paths to each S957 fit has been assessed using the variation of the F-test. Before the addition of the extra U-S scattering path the R-factors for the non-saline and saline fits were 0.0202 and 0.0212, these then became 0.0170 and 0.0155 respectively upon the addition of the path. Calculated α values for this were 53% and 75%. This tells us that the addition of the extra U-S path in the non-saline environment does not improve the fit significantly, whereas it does in the saline environment. So we are able to conclude that an aqueous sulfate group is associated with the resin-uranyl complex in saline conditions most of the time, whereas it is less definitive for the non-saline environment, and therefore less likely to be found associated with the bound uranyl.

This suggests that there is binding to the uranyl by a resin based phosphonate group, but it was unclear whether the sulfur atoms were from a resin based sulfonate, aqueous sulfate group or a combination thereof. Fits are shown in Figure 8, with fitting parameters being shown in Table 10.

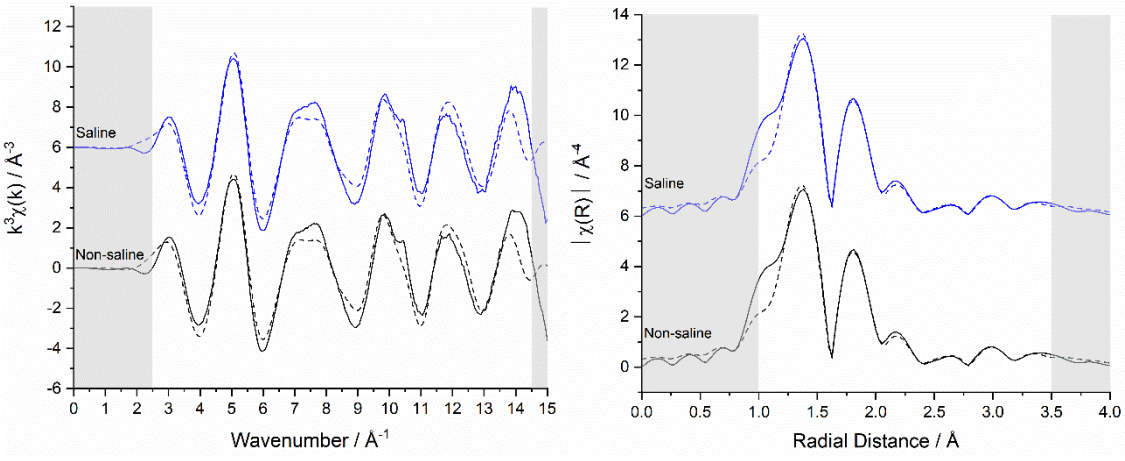

Figure 8. Uranium L_{III}-edge EXAFS spectra in R- and K-space for uranyl loaded Purolite S957 from non-saline (A) and saline (B) environments, fit with uranyl bound in a monodentate manner to a sulfonate and a phosphonate group and a

bidentate sulfate. The unshaded region represents the fitting window, solid and dashed lines show the data and fits, respectively.

Table 10. U L_{III}-edge EXAFS fitting parameters of data from uranyl loaded Purolite S957 from non-saline and saline conditions. *Values linked to other multiple scattering (MS) paths and were parameterised accordingly.

	Scattering Path	N	R / Å	σ^2	dE_0 / eV	amp	R-Factor
Non-Saline	U-O_{axial}	2	1.79	0.00267	1.815	1.039	0.0140
	U-$O_{equatorial}$	2	2.46	0.00199			
	U-$O_{equatorial}$	2	2.33	0.00106			
	U-P	1	3.56	0.00846			
	U-S	1	3.30	0.00381			
	U-S	1	3.12	0.00707			
	U-$O_{sulfate}$	2	4.01	0.0324			
	U-O_{axial} (MS)	2	3.57*	0.00534*			
	U-O_{axial} (MS)	2	3.57*	0.00534*			
Saline	U-O_{axial}	2	1.79	0.00265	1.787	1.034	0.0148
	U-$O_{equatorial}$	2	2.46	0.00698			
	U-$O_{equatorial}$	2	2.32	0.00120			
	U-P	1	3.40	0.01923			
	U-S	1	3.27	0.00367			
	U-S	1	3.09	0.00472			
	U-$O_{sulfate}$	2	4.04	0.00323			
	U-O_{axial} (MS)	2	3.58*	0.00544*			
	U-O_{axial} (MS)	2	3.58*	0.01089*			

Purolite S957 has been fit with the same model in both non-saline and saline environments. The bond lengths infer a chelated uranyl molecule which is 4-coordinate in the equatorial plane, with oxygen atoms from both phosphonate and sulfur containing groups on the resin being involved. The non-innocence of resin based phosphonate and sulfonate groups during uranyl binding by Purolite S957 has been reported, via comparison of IR spectra for the loaded and non-loaded resin.[24]

U-P distances are 3.56 and 3.40 in non-saline and saline environments, respectively, with previously reported examples of uranyl-phosphonate compounds in the solid state having monodentate U-P distances between 3.47 and 3.76 Å.[25–27] Bidentate phosphonate U-P distances tend to be between 3.13 and 3.16 Å.[26,27] This is considerably shorter than what

was found for uranyl bound to S957 in both saline and non-saline environments, suggesting the phosphonate moiety binds the uranyl cation in a monodentate fashion. The slightly shorter measured U-P distance of 3.40 Å for the saline environment may suggest the presence of some bidentate phosphonate coordination. However, from looking at the differences in the interatomic distances between the two possibilities it is clear that the monodentate binding mode is dominant. However, the position of the sulfonate group, either *meta*- or *ortho*- relative to the phosphonate group, is not explicitly known. The two different possibilities may produce different binding modes.

The assignment of sulfur atoms to the bidentate or monodentate binding modes of sulfonate or sulfate moieties is challenging. U-S monodentate interatomic distances have been reported at around 3.6 Å, with bidentate U-S distances having been reported at around 3.1 Å (in both aqueous and solid phase).[12,22,23] U-S distances from the fits clearly show, for both environments, that one of the S atoms is associated with a bidentate sulfate/sulfonate group (U-S distances = 3.12 and 3.09 Å for non-saline and saline respectively). The other U-S distance is more problematic to define, with the distances of 3.30 and 3.27 Å for non-saline and saline environments, respectively, being between reported examples for monodentate and bidentate coordination of sulfonate to uranyl.[12,22,23] As discussed above, the position of the sulfonate group on the benzene ring will affect its binding mode towards uranyl, and this suggests a mix of monodentate and bidentate coordination, and the EXAFS signal is an average thereof. However, a similar argument can be made for the second S atom, assumed to be associated with an aqueous sulfate group, where it could be binding in either coordination mode depending on local solution conditions and steric effects associated with the solid resin.

3.6. Mechanisms: Ion Exchange vs. Chelation

The extraction mechanisms of novel ion exchange resin functionalities reported in the literature are often not directly determined, rather, they are inferred either from crystal structure data and/or knowledge of ligand-metal coordination behaviour. For example, IX resins with ethylenediaminetris(methylenephosphonic) acid, pentaethylenehexamine, N,N'-dimethy-N,N'-dibutylmalonamide, phosphonamidic acid and succinic acid are all reported as extracting uranium from the aqueous phase via a chelation mechanism, but this has not been experimentally determined.[28–32]

Polyamine resins are generally considered to function as WBA resins, even though it would be theoretically possible for purely aminic molecules to directly bind to the uranyl cation via the nitrogen lone pair.[7] This anion exchange mechanism has been supported by the extracted $[UO_2(SO_4)_3]^{4-}$ species reported from EXAFS data in this paper and the literature.[9] This has implications when choosing a WBA resin for uranium recovery, as the aqueous environment must enable to formation of anionic uranyl complexes.

This anion exchange mechanism suggests that these resins may not be suitable for uranium extraction from saline environments where $[Cl]^-$ = 22.7g L^{-1}, as uptake suppression is likely to happen. This has been observed by Ogden *et al.*, where uranyl uptake was supressed as $[Cl]^-$ increased from 0 to 70 g L^{-1}, however, at $[Cl]^-$ > 70 g L^{-1} uptake was seen to increase, likely due to the formation and extraction of U-chloro species by Dowex Monosphere 77.[6] This is much higher than the chloride concentrations used in this study, and suggests the possibility of a process involving uranium extraction from brines with $[Cl]^-$ in excess of 100 g L^{-1}. Such high levels of chloride may have negative effects further on in the process, particularly with contamination of the uranium product.

The uranyl cation is well known to form solid and solution phase complexes with N-donor ligands, prompting the question: why does uranyl not directly bind to the bispicolylamine functionality?[33,34] M4195 is marketed as a chelating resin for copper, nickel and cobalt processing. Though there has been no direct measurement to assess the binding mode of a bispicolylamine resin towards Cu^{2+}, Ni^{2+} and Co^{2+}, experimental data does suggest that this is the case.[35,36] At the salinity used by Diniz *et al.* ($[Cl]^-$ = 3.6 M) Cu^{2+}, Ni^{2+} and Co^{2+} speciation is dominated by the bare cation and monoanionic chloride species (calculated using stability constants).[35] This leads to the conclusion that the uptake mechanism cannot be based purely on electrostatics, and an anion exchange mechanism is unlikely to be the dominant extraction process.

The ability of the nitrogen atoms in the BPA functional group to bind directly to metals will be highly dependent on the size of the metal due to the conformation of the BPA group, and restrictions on conformational flexibility due to the effects of tethering to the resin. The crystal ionic radii of Cu^{2+}, Ni^{2+} and Co^{2+} are 0.72, 0.72 and 0.74 Å respectively, with that for uranyl being 1.4 Å.[35,37,38] As the ionic radius for the uranyl cation is significantly larger than those which form chelates with BPA it can be inferred that this anion exchange mechanism arises in part due to steric effects overcoming the enthalpic benefit of chelate formation.

Another point to note is that the uranyl cation behaves as a hard acceptor according to HSAB theory and forms weaker complexes with nitrogen donor ligands than oxygen donors, such as sulfate.

This difference in mechanism suggests that aqueous cations such as Cu^{2+}, Ni^{2+} and Co^{2+} would likely be preferentially removed from solution over uranyl. So Dowex M4195 may not be suitable for uranyl recovery from aqueous systems containing first row transition metals, however, if uranium is the contaminant in such systems then this is a positive characteristic. Additionally, after removal of first row transition metals the aqueous phase could be treated to remove any uranium present, providing both environmental and potential economic benefits towards miner processing flowsheets.

Amidoxime functionalised solids are usually discussed within the remit of uranium extraction from seawater, with their use being attributed to high uranyl loading capacities from seawater arising from a chelation extraction mechanism.[17,39–42] However, apart from work by Abney *et al.*, understanding of the binding mode upon uranyl extraction has come from computational and single crystal x-ray diffraction experiments.[17] Computational studies suggest that the η^2 binding mode is the most thermodynamically stable mode, though EXAFS fits by Abney *et al.* have determined a chelated uranyl environment, with a co-extracted μ^2-oxo-bridged transition metal element.[17,43] This disagreement between computational and experimental results presented here and in the literature show that it is currently not possible to predict exact uranyl coordination environment and therefore extraction mechanism with regards to amidoxime functionalised solids. A large factor in these differences likely arises from steric effects due to the binding of the amidoxime moiety to the solid support, something which needs to be understood to allow for the design and implementation of more effective amidoxime based uranyl extractants. A point not often discussed is that the nitrogen atom can become protonated, which could lead to an anion exchange mechanism, depending on solution conditions.

Purolite S957 contains sulfonic acid groups, and is therefore theoretically capable of extracting uranium from aqueous solutions via a cation exchange process. This is also theoretically possible with the phosphonic acid groups as well, but has not been reported in the literature. This has implications for uranyl recovery processes where there are other cationic species present in solution (Na^+, Mg^{2+}, Ni^{2+}, Eu^{3+}, etc), as these may also be extracted. However, the EXAFS data reported here for S957 suggest a chelation extraction mechanism,

which would likely outcompete a cation exchange process, implying S957 may be appropriate for uranyl recovery from a variety of aqueous matrices.

4. Conclusions

A set of ion exchange resins consisting of various functionalities that are capable of chelating to metal ions have been analysed using EXAFS to determine their binding mode towards uranyl loaded from non-saline and saline conditions analogous to sea water environments. It has been shown that the presence of chloride has little effect on uranyl binding mode by all studied resins.

Dowex M4195 and WBA resins Ps-EDA, Ps-DETA, Ps-PEHA and Purolite S985 were fit with the extracted species being $[UO_2(SO_4)_3]^{4-}$. This species is generally accepted for uranyl extraction onto strong base anion exchange resins in conventional uranium mining process flow sheets. The prevalence of an anion exchange mechanism as opposed to chelation implies that this resin type may be unsuitable for U recovery from high saline environments, as is the case with conventional SBA resins.

Purolite S910 exhibited a binding mode involving two amidoxime groups from the resin. This has been observed previously, with other uranyl extractants showing this behaviour as well.[17,44,45] Fitting data suggests that there is more than one binding mode present, with U-N and U-C interatomic distances fitting in between previously reported values for monodentate and η^2 binding modes. The fits do not explicitly show that there are only chelated U environments present, as different amidoxime groups may bind UO_2^{2+} in a monodentate fashion. The likely scenario is that there is a mixture of binding modes present on the surface of the resin. This result is further evidence that the binding of uranyl by amidoxime functionalised solids is not simple and is highly dependent on factors such as steric hindrance and reduced flexibility imparted through tethering.

Purolite S957 was the only resin in this study to be successfully fit with a chelation model, involving both sulfonate and phosphonate functionalities present on the resin, and a 4-coordinate equatorial plane. Again, it was difficult to determine the precise coordination mode of the sulfonate and phosphonate groups, though it is likely to be a mixture of bidentate and monodentate for both. The presence of a further sulfur atom from a sulfate group cannot be known with absolute certainty for this resin, though the F-test used does suggest that in saline conditions this sulfur atom is present the majority of the time.

This knowledge of uranyl coordination environment and binding mode can be implemented to design future uranium extraction flowsheets which are tolerant to saline conditions. Further to this, understanding how different tethered functionalities interact with the uranyl cation on a molecular level could be used in the design of new, selective extractants which are effective in systems containing lower quality waters.

5. Acknowledgements

The authors would like to thank the EPSRC for funding this work (EPSRC reference: EP/G037140/1), the Diamond Light Source for the opportunity to run these experiments (SP12643-1), the B-18 principal beamline scientist Dr. Giannantonio Cibin for his help with data acquisition, Professor Katherine Morris at the Research Centre of Radwaste and Decommissioning for assistance with sample preparation and the University of Sheffield for provision of uranyl sulfate.

6. References

1 International Atomic Energy Agency, *Energy, Electricity and Nuclear Power Estimates for the Period up to 2050*, Vienna, 2015.
2 K. Soldenhoff, in *ALTA*, 2006.
3 A. Taylor, *Short Course in Uranium Ore Processing*, ALTA Metallurgical Services Publications, 2016.
4 N. Kabay, M. Demircio lu, S. Yaylı, E. Gu, M. Yu, M. Sa lam and M. Streat, *Ind. Eng. Chem. Res.*, 1998, **37**, 1983–1990.
5 J. Kim, C. Tsouris, R. T. Mayes, Y. Oyola, T. Saito, C. J. Janke, S. Dai, E. Schneider and D. Sachde, *Sep. Sci. Technol.*, 2013, **48**, 367–387.
6 E. M. Moon, M. D. Ogden, C. S. Griffith, A. Wilson and J. P. Mata, *J. Ind. Eng. Chem.*, 2017, **51**, 255–263.
7 E. J. Zaganiaris, *Ion Exchange Resins in Uranium Hydrometallurgy*, Books on Demand France, 2009.
8 G. R. Choppin and M. P. Jensen, in *The Chemistry of the Actinide and Transactinide Elements*, eds. L. R. Morss, N. M. Edelstein and J. Fuger, Springer, Netherlands, 4th edn., 2010, p. 2524.
9 J. T. M. Amphlett, M. D. Ogden, R. I. Foster, N. Syna, K. H. Soldenhoff and C. A. Sharrad, *Chem. Eng. J.*, 2018, **334**, 1361–1370.
10 L. Downward, C. H. Booth, W. W. Lukens and F. Bridges, *AIP Conf. Proc.*, 2007, **882**, 129–131.
11 W. C. Hamilton, *Acta Cryst*, 1965, **18**, 502–510.
12 C. Hennig, K. Schmeide, V. Brendler, H. Moll, S. Tsushima and A. C. Scheinost, in *13th International Proceedings on X-Ray Absorption Fine Structure*, Stanford, 2006, pp. 262–264.
13 R. M. Smith, A. E. Martell and R. J. Motekaitis, in *NIST Standard Reference Database 46*, Gaithersburg, MD, 2004.
14 M. Walter, T. Arnold, T. Reich and G. Bernhard, *Environ. Sci.*, 2003, **37**, 2898–2904.
15 M. D. Ogden, E. M. Moon, A. Wilson and S. E. Pepper, *Chem. Eng. J.*, 2017, **317**, 80–89.
16 M. D. Ogden, E. M. Moon, A. Wilson, C. Griffith, J. Mata, K. Soldenhoff and S. E. Pepper, *Chem. Eng. J.*, 2017, **324**, 414.
17 C. W. Abney, R. T. Mayes, M. Piechowicz, Z. Lin, V. S. Bryantsev, G. M. Veith, S. Dai and W. Lin, *Energy Environ. Sci.*, 2016, **9**, 448–453.
18 E. G. Witte, K. S. Schwochau, G. Henkel and B. Krebs, *Inorganica Chim. Acta*, 1984, **94**, 323–331.
19 G. Tian, S. J. Teat, Z. Zhang and L. Rao, *Dalt. Trans.*, 2012, **41**, 11579.
20 S. Vukovic, L. A. Watson, S. O. Kang, R. Custelcean and B. P. Hay, *Inorg. Chem.*, 2012, **51**, 3855–3859.

21 D. M. Sherman, C. L. Peacock and C. G. Hubbard, *Geochim. Cosmochim. Acta*, 2008, **72**, 298–310.
22 A. Zalkin, H. Ruben and D. H. Templeton, *Inorg. Chem.*, 1978, **17**, 3701–3702.
23 M. B. Doran, A. J. Norquist and D. O'Hare, *Acta Crystallogr. Sect. E Struct. Reports Online*, 2003, **59**, m762–m764.
24 V. M. Gelis, V. V. Milyutin, E. A. Kozlitin, N. A. Nekrasova and Y. V. Shumilova, in *Waste Management 2011*, Pheonix, Arizona, 2011.
25 W. Yang, T. Tian, H. Y. Wu, Q. J. Pan, S. Dang and Z. M. Sun, *Inorg. Chem.*, 2013, **52**, 2736–2743.
26 C. Liu, W. Yang, N. Qu, L. J. Li, Q. J. Pan and Z. M. Sun, *Inorg. Chem.*, 2017, **56**, 1669–1678.
27 J. A. Danis, W. H. Runde, B. Scott, J. Fettinger and B. Eichhorn, *Chem. Commun.*, 2001, **5**, 2378–2379.
28 A. Kadous, M. A. Didi and D. Villemin, *J. Radioanal. Nucl. Chem.*, 2010, **284**, 431–438.
29 S. A. Sadeek, E. M. M. Moussa, M. A. El-Sayed, M. M. Amine and M. O. Abd El-Magied, *J. Dispers. Sci. Technol.*, 2014, **35**, 926–933.
30 S. A. Ansari, P. K. Mohapatra and V. K. Manchanda, *Talanta*, 2007, **73**, 878–885.
31 O. Abderrahim, M. A. Didi and D. Villemin, *J. Radioanal. Nucl. Chem.*, 2009, **279**, 237–244.
32 P. Metilda, K. Sanghamitra, J. Mary Gladis, G. R. K. Naidu and T. Prasada Rao, *Talanta*, 2005, **65**, 192–200.
33 S. C. Bart and K. Meyer, *Highlights in Uranium Coordination Chemistry*, Springer Berlin Heidelberg, 2008, vol. 127.
34 J. L. Sessler, P. J. Melfi and G. D. Pantos, *Coord. Chem. Rev.*, 2006, **7**–**8**, 816–843.
35 C. V. Diniz, F. M. Doyle and V. S. T. Ciminelli, *Sep. Sci. Technol.*, 2002, **37**, 3169–3185.
36 R. R. Grinstead, in *Ion Exchange Technology*, Ellis Horwood Ltd, London, 1984, pp. 509–518.
37 C. Gupta and H. Singh, *Uranium Resource Processing: Secondary Resources*, Springer-Verlag Berlin Heidelberg, 1st edn., 2003.
38 R. D. Shannon, *Acta Crystallogr. Sect. A*, 1976, **32**, 751–767.
39 S. H. Choi, M. S. Choi, Y. T. Park, K. P. Lee and H. D. Kang, *Radiat. Phys. Chem.*, 2003, **67**, 387–390.
40 H. J. Schenk, L. Astheimer, E. G. Witte and K. Schwochau, *Sep. Sci. Technol.*, 1982, **17**, 1293–1308.
41 J. Kim, Y. Oyola, C. Tsouris, C. R. Hexel, R. T. Mayes, C. J. Janke and S. Dai, *Ind. Eng. Chem. Res.*, 2013, **52**, 9433–9440.
42 J. Kim, C. Tsouris, R. T. Mayes, Y. Oyola, T. Saito, C. J. Janke, S. Dai, E. Schneider and D. Sachde, *Sep. Sci. Technol.*, 2013, **48**, 367–387.
43 S. Vukovic, L. A. Watson, S. O. Kang, R. Custelcean and B. P. Hay, *Inorg. Chem.*, 2012, **51**, 3855–3859.
44 M. Carboni, C. W. Abney, S. Liu and W. Lin, *Chem. Sci.*, 2013, **4**, 2396–2402.
45 L. Zhou, M. Bosscher, C. Zhang, S. Özçubukçu, L. Zhang, W. Zhang, C. J. Li, J. Liu, M. P. Jensen, L. Lai, C. He, S. Ozcubukcu, L. Zhang, W. Zhang, C. J. Li, J. Liu, M. P. Jensen, L. Lai and C. He, *Nat Chem*, 2014, **6**, 236–241.